Dynamics of N6-methyladenosine modification during Alzheimer's disease development

Yuqing Wang
Jinzhou Medical University
Xiaoyu Li
Fudan University
Baozhi Yang
Jinzhou Medical University
Ti-Fei Yuan
Shanghai Mental Health Center
Bo Peng
Fudan University
Yanxia Rao (yanxiarao@connect.hku.hk)
Fudan University

Research Article

Keywords: Alzheimer's disease, N6-methyladenosine, ALKBH5, METTL3, microglia, WTAP

Posted Date: April 28th, 2023

DOI: https://doi.org/10.21203/rs.3.rs-2861775/v1

Abstract

N6-methyladenosine (m6A) modification is a common RNA modification in the central nervous system and has been linked to various neurological disorders, including Alzheimer's disease (AD). However, little is known about the dynamic of mRNA m6A modification and m6A enzymes during the development of AD.Therefore, this study examined the expression profiles of m6A and its enzymes in the development of AD. The results showed that changes in the expression levels of m6A regulatory factors occurred in the early stages of AD, indicating the potential involvement of m6A modification in disease onset. Moreover, the analysis of mRNA m6A expression profiles using m6A-seq revealed significant differences in m6A modification between AD and control brains.The differentially methylated genes were enriched in GO and KEGG terms related to processes such as inflammation response, immune system processes. And the differently expressed genes (DEGs) are negative associated with microglia homeostasis genes and but positive for “disease-associated microglia” (DAM) associated genes, suggesting that dysregulation of mRNA m6A modification may contribute to the development of AD by affecting the function and gene expression of microglia.

Introduction

Alzheimer's disease (AD) is a neurodegenerative disorder in the central nervous system (CNS) that lead to dementia, being the most common cause of dementia in the elderly[1]. The pathological changes of AD mainly involve the deposition of β-amyloid (Aβ) to form plaques and the formation of neurofibrillary tangles (NFTs), in which the microtubule-associated protein tau plays a major role and eventually leads to neuronal damage[2]. Environmental exposure and genetic susceptibility are risk factors for AD[3]. However, the heterogeneity pathologies of AD among individuals with similar or identical susceptibility genes suggests the involvement of epigenetics in the disease.

Epigenetics refers to the heritable phenotype changes that occur without changes in the DNA sequence, which is different from genetics, which is caused by changes in the nucleotide sequence. Epigenetics includes DNA methylation, histone modification, chromatin remodeling, and non-coding RNA regulation. N6-methyladenosine (m6A) is a widely occurring methylation modification on mRNA, which occurs at the sixth nitrogen atom of adenine[4]. This modification is dynamically reversible, and the regulatory factors involved in m6A methylation modification include "Writers" (methyltransferases), "Erasers" (demethylases), and "Readers" (binding proteins) of m6A[5]. The main components of methyltransferase complex (MACOM) are methyltransferase-like 3 (METTL3), methyltransferase-like 14 (METTL14), and Wilms tumor 1-associated protein (WTAP), which cooperate with each other to perform catalytic functions[6, 7]. Demethylases include fat and obesity-associated protein (FTO) and ALKB homolog 5 (ALKBH5)[8, 9], while m6A methylation binding proteins include various binding proteins containing YTH domains[10], heterogeneous nuclear ribonucleoproteins (hnRNPs)[11], and eukaryotic initiation factor 3 (eIF3)[12]. The study by Miao et al[13] has found that m6A modification is not random, and its content is related to the length and number of exons and the distance from neighboring genes. Recent studies have

revealed that epigenetic modifications can affect the development of the nervous system, such as neurogenesis, axon growth, synaptic plasticity, circadian rhythm, cognitive function, and stress response[14–16]. When the expression patterns of genes controlled by epigenetics are dysregulated, it may lead to autoimmune diseases, cancer, and various other diseases. m6A-related proteins are widely expressed in neurons and regulate neurogenesis, memory formation and consolidation, cerebellar development, and axon regeneration[17–19]. Moreover, m6A modification abnormalities have been found in various neurodegenerative diseases, including AD[20, 21].

It is worth noting that although many studies have reported changes in m6A in AD, including alterations in METTL3, METTL14, and FTO, the dynamics of m6A and m6A enzymes during AD development remain unclear[22, 23]. To this end, we analyzed m6A methylation levels in hippocampal brain tissues from 5xFAD transgenic mice at different ages, and used real-time quantitative PCR (RT-qPCR) to investigate the expression of m6A regulatory factors during different stages of AD progression. We also employed immunofluorescence staining to investigate the association of methyltransferases METTL3 and WTAP with Aβ, and applied mRNA m6A methylation sequencing (MeRIP-seq or m6A-seq) technology to investigate the changes in m6A modification at the genome-wide level during the AD process. These findings may offer a new perspective for understanding the potential role of m6A modification in AD pathogenesis and identifying new therapeutic targets for AD treatment.

Materials and methods

Animals

5xFAD(B6.Cg-Tg(APPSwFlLon,PSEN1M146LL286V)6799Vas/Mmjax, Stock No: 008730) mice was purchased from The Jackson laboratory. They were used in this study alongside their wild-type littermates at 3, 6, and 9 months of age. The mice were housed in a 12-hour light/dark cycle and kept at a constant temperature of 22–24℃. Food and water were provided ad libitum.

Tissue preparation for RNA extraction and immunohistochemistry

To obtain brain tissue for analysis, mice were anesthetized and perfused with either 50 ml of 0.01M cold PBS or 0.9% Nacl. The right hemisphere was used to collect hippocampal tissue, which was flash-frozen in dry ice and stored at -80°C prior to cryosection. Tissue RNA samples were extracted using the manufacturer's protocol (Takara, Cat# 9767). The left hemisphere was postfixed in 4% paraformaldehyde (PFA) overnight and then dehydrated with 30% sucrose in 0.01 M PBS at 4°C for 2–3 days. Finally, the tissues were embedded in optimal cutting temperature compound (OCT) and stored at -80°C before cryosection.

Quantification of the m6A Modification

In this study, we used the m6A RNA Methylation Quantification Kit (Epigentek, Cat# P-9005)to measure the m6A content in the total RNAs. In this assay, total RNA is bound to strip wells using a RNA high binding solution. m6A is detected using specific capture and detection antibodies. The detected signal is enhanced and then quantified colorimetrically by reading the absorbance in a microplate spectrophotometer at a wavelength of 450 nm. The total amount of RNA in each reaction was 300 ng. RNA m6A relative quantification assay was performed following the manufacturer's protocol.

Quantitative Real-Time PCR

Genomic DNA was removed from total RNA and cDNA was rapidly synthesized through PrimeScript™ RT reagent Kit with gDNA Eraser (Takara, Cat# RR047A). TB Green® Premix Ex Taq™ (Tli RNaseH Plus) (Takara, Cat# RR420A) and a LightCycler480 System (Roche Diagnostics) were used for qRT-PCR. Gapdh was used as internal control, relative expression of the following genes, *Ythdf1*, *Ythdf2*, *Ythdf3*, *Ythdc1*, *Mettl3*, *Mettl14*, *Wtap*, *Fto* and *Alkbh5*, were calculated using the 2-ΔΔCt method. Details of primer sequences used in the study are shown in supplementary table 6.

Immunohistochemistry

All tissues were frozen in the freezing microtome for 15 minutes before cryosection. Coronal sections of the brain were made at a thickness of 30 μm by Leica CM1950 cryostat and rinsed by 0.01M PBS for 3 times. Brain were blocked and permeabilized with 0.01M PBS containing 0.3% Triton X-100 and 4% normal donkey serum (NDS) for 2 hours at room temperature (RT). Next, the samples were incubated in primary antibody diluted 1%NDS in PBST at 4 ° C ON. After rinsed by 0.01M PBS 10 minutes for 3 times, the secondary antibody was incubated for 2 hours at RT, together with 4’,6-diamidino-2-phenylindole (DAPI, 1:1000). Next, samples are rinsed by 0.01M PBS for 3 times and then mounted anti-fade mounting medium. Then sealed the edge of the cover glass with nail enamel.

Primary antibodies included the following: Rabbit anti-METTL14 (sigma, Cat# HPA038002 1:500); Rabbit anti-YTHDF3 (Proteintech, Cat# 25537-1-AP 1:500); Rabbit anti-ALKBH5 (Millipore, Cat# ABE547 1:500); Goat anti-IBA1 (Abcam, Cat# ab5076 1:500); Goat anti-Olig2 (Biotechne, Cat# AF2418-SP 1:500); Rabbit anti-YTHDF1 (Proteintech, Cat# 17479-1-AP 1:500); Rabbit anti-YTHDF2 (Proteintech, Cat# 24744-1-AP 1:500); Rabbit anti-WTAP (Proteintech, Cat# 10200-1-AP 1:500); Rabbit anti-m6A (synaptic systems, Cat# 202003 1:500); Rabbit anti-METTL3 (Abcam, Cat# ab195352 1:500); Mouse anti-β-Amyloid (Biolegend, Cat# 803014 1:2000); Mouse anti-NeuN (Abcam, Cat# ab104224 1:1000); Mouse anti-GFAP (Sigma, Cat# G3893 1:500). Secondary antibodies included the following: AlexaFluor-488-, AlexaFluor-555-, or AlexaFluor-647-conjugated secondary antibodies against goat, rabbit, mouse (Invitrogen, 1:1000) antibodies.

MeRIP-seq

Total RNA was isolated and purified using TRIzol reagent (Invitrogen, Carlsbad, CA, USA) following the manufacturer's procedure. The RNA amount and purity of each sample was quantified using NanoDrop ND-1000 (NanoDrop, Wilmington, DE, USA), and the RNA integrity was assessed by Bioanalyzer 2100

(Agilent, CA, USA). Poly (A) RNA was purified from 50μg total RNA using Dynabeads Oligo (dT)25-61005 (Thermo Fisher, CA, USA) by two rounds of purification. Then the poly(A) RNA was fragmented into small pieces using Magnesium RNA Fragmentation Module (NEB, cat.e6150, USA) under 86℃ 7min. The cleaved RNA fragments were incubated for 2h at 4℃ with m6A-specific antibody (No. 202003, Synaptic Systems, Germany) in IP buffer (50 mM Tris-HCl, 750 mM NaCl and 0.5% Igepal CA-630). The IP RNA was reverse-transcribed to cDNA by SuperScript™ II Reverse Transcriptase (Invitrogen, cat. 1896649, USA), which was next used to synthesise U-labeled second-stranded DNAs with E. coli DNA polymerase I (NEB, cat.m0209, USA), RNase H (NEB, cat.m0297, USA) and dUTP Solution (Thermo Fisher, cat.R0133, USA). An A-base was added to the blunt ends of each strand, preparing for ligation to the indexed adapters. Dual-index adapters were ligated to the fragments, and size selection was performed with AMPureXP beads. After the heat-labile UDG enzyme (NEB, cat.m0280, USA) treatment of the U-labeled second-stranded DNAs, the ligated products were amplified with PCR by the following conditions: initial denaturation at 95℃ for 3 min; 8 cycles of denaturation at 98℃ for 15 sec, annealing at 60℃ for 15 sec, and extension at 72℃ for 30 sec; and then final extension at 72℃ for 5 min. At last, we performed paired-end sequencing (PE150) on an Illumina Novaseq™ 6000 platform(LC-Bio Technology CO., Ltd., Hangzhou, China) following the vendor's recommended protocol.

MeRIP-seq data analysis

The quality of IP and Input sample sequences was assessed using FastQC and RseQC. Low-quality reads and those containing adaptors were removed using fastp (v0.19.4) with default settings. Reads were mapped to the reference genome (mm10) using HISAT2 (v2.0.4). Peak calling and differential peak analysis were conducted in R (v4.2.2) using the exomePeak package (v2.16.0). Peak annotations were performed with ANNOVAR. De novo and known motif discovery, as well as motif localization relative to the peak summit, were carried out using MEME and HOMER (v4.10). Transcript and gene expression levels were determined from input libraries using StringTie (v2.1.2) by calculating FPKM (total exon fragments/mapped reads (millions) x exon length (kB). Differential analysis was based on the FPKM matrix and performed using edgeR (v3.40.2) with quasi-likelihood (QL) F-tests. Genes with an absolute log2(fold change) greater than log2 (1.5) and a p-value less than 0.05 were considered as significant differentially expressed genes (DEGs). Volcano plots were created using the EnhancedVolcano package (v1.16.0). Gene Ontology (GO) and KEGG pathway analyses were conducted using the enrichGO and enrichKEGG functions of the clusterProfiler package (v4.6.2). Categories with a false discovery rate (FDR) of 0.05 or lower were deemed significantly enriched, and these categories were visualized using ggplot2 (v3.4.2). Detailed information can be found in the accompanying R script.

Statistical Analysis

Statistical analysis was performed using GraphPad Prism (GraphPad Software, Version 8.0, La Jolla, USA). Each data point represented the average statistical result of three sections in different regions of the brain. Results were determined independently at double-blind manner. All data were shown as mean ± standard deviation (SD) (bar plot). Data from multiple groups were evaluated statistically by one-way

analysis of variance (ANOVA) with Holm-Sidak's multiple comparisons test (post hoc). Student's t test was used for comparison between the two groups. Statistical significance was set as $P < 0.05$.

Results

Aβ plaque accumulation is associated with mRNA m6A modification

To investigate the changes in mRNA m6A levels during the progression of AD, we performed m6A detection in the hippocampal from 5xFAD and age-matched wild-type (WT) mice. The 5xFAD mouse model begins to express a significant amount of Aβ42 at 2 months of age, leading to the development of pathological features such as amyloid-like protein accumulation and glial hyperplasia[24]. These mice exhibit a deterioration in learning and memory at the age of 6 months old and neuronal apoptosis at the age of 9 months old[24]. Therefore, we analyzed the m6A level at four time points, including 1-month (1 mo), 3-month (3 mo), 6-month (6 mo), and 9-month (9 mo). We observed a gradual decrease in m6A levels in both 5xFAD and WT mice as they aged. However, no significant difference was detected in the total m6A levels between 5xFAD and WT mice at the various timepoints (Fig. 1A). We then investigated the expression profiles of m6A in neuron, microglia, oligodendrocytes, and astrocytes during AD progression by co-staining cell-specific markers with m6A (Fig. 1B and sFig.1). The m6A antibody was used to identify and quantify the presence of m6A modification in RNA molecules. We found that m6A was highly expressed in neurons than glial cells in the adult mouse brain (Fig. 1B). However, no significant differences in total m6A expression were observed between AD and control groups across aging (Fig. 1C).

The accumulation of Aβ plays a central role in the pathogenesis of AD, which contributes to neuronal dysfunction and neurodegeneration. Several mechanisms have been proposed to explain the impact of Aβ on neuronal function, including synaptic dysfunction, oxidative stress and inflammation, mitochondrial dysfunction, neuronal death and tau hyper phosphorylation [25, 26]. But, the impact of Aβ aggregation on mRNA m6A modification remains illusive. To this end, we examine the distribution of Aβ plaques and m6A profiles using immunofluorescence (Fig. 1D-1F). Next, we quantified the fluorescence intensity of m6A around Aβ and non-Aβ regions. The results showed that the levels of m6A surrounding Aβ plaques were significantly lower compared to the non-Aβ region and control brain, as early as 3 months of age (Fig. 1D).

Profiles the m6A enzymes expression in the adult brain.

The observed reduction in m6A levels surrounding Aβ plaques suggested a potential link between Aβ plaques formation and alterations in mRNA m6A modification during AD development. To further explore this relationship, We examined the features of YTH domain family proteins, including YTHDF1, YTHDF2, YTHDF3, and YTHDC1, which are involved in reading methylated RNA; methyltransferases METTL3,

METTL14, and WTAP; and demethylases ALKBH5 and FTO in normal and AD brain. We firstly assessed the expression of these m6A enzymes in neurons and glial cells using whole brain scRNA-seq data from adult mouse brain (YX Li, unpublished data). We observed that *Ythdf1 ~ 3*, *Ythdc1*, *Igf2bp3*, *Mettl3*, *Mettl14, Wtap*, *Alkbh5*, and *Fto* were abundantly expressed in 16 populations identified, except for hemoglobin-expressing vascular cells (Hb-VC) (sFig2). All regulatory factors were highly enriched in neurons, including mature neuron (mNEUNR), immature neuron (ImmN) and neuroendocrine cell (NendC) (Fig. 2A, 2E, 2I and sFig.2). Additionally, *Ythdf2*, *Ythdf3*, *Wtap*, *Alkbh5* and *Fto* were highly expressed in glial cells, such as astrocytes, oligodendrocytes, and microglia (Fig. 2A, 2E, 2I and sFig.2).

Next, we further investigated the cellular localization of these regulatory factors in the adult mouse brain using immunofluorescence. The m6A regulatory factors, including writers (METTL3, METTL14 and WTAP), erasers (FTO and ALKBH5), and readers (YTHDF1, YTHDF2 and YTHDF3), were co-stained with the neuronal and glia cell markers. We found that these m6A regulatory factors were widely and strongly expressed in neurons within the hippocampus and cortex of the adult mouse brain in the steady state (Fig. 2). In contrast to observation from scRNA-seq, these proteins were hardly detectable in glia cells under the steady-state condition (sFig.3, sFig4 and sFig5).

Dynamic changes of m6A-related regulatory factors in the progression of Alzheimer's disease

Next, we investigated the alterations in m6A-related regulatory factors at the RNA level during different stages of AD progression. Firstly, we analyzed published mouse bulk RNA-seq data, focusing on the dynamic changes of m6A enzymes during the development of AD [27]. We found that *Wtap* exhibited significant downregulation in expression during the early stage of AD (4-month-old), whereas *Ythdc1*, *Ythdf3*, and *Fto* showed significant changes in expression in the later stage of AD (18-month-old) compared to control samples (sFig. 6).

In this study, we conducted RT-qPCR experiments on total RNA extracted from the hippocampus of adult mice at 1, 3, 6, and 9 months of age (Fig. 3 and supplementary table 1). In the early stages of AD, we have observed a marked alteration in a number of m6A-related enzymes, including *Mettl3*, *Wtap*, *Ythdf1*, *Ythdc1*, and *Alkbh5* (Fig. 3 and supplementary table 1). Previous studies have demonstrated that YTHDF2 involved in regulating hippocampal dentate gyrus-dependent learning and memory [28]. YTHDF3 has to be shown to be correlated with cognitive recovery[29]. At 6 months, *Ythdf2* and *Ythdf3* expression were significantly downregulated in the 5xFAD group compared to the WT group ($P < 0.05$), *Ythdc1* expression was also downregulated in the 5xFAD group (Fig. 3C). Unexpectedly, there were no significant differences in the expression levels of the proteins involved in mRNA m6A methylation modification between the 5xFAD and WT control groups ($P > 0.05$) at 9 months of age (Fig. 3). The changes in *WTAP* that we observed at 3 months of age were consistent with the previous sequencing data, indicating that alterations in m6A enzymes indeed occur early on during AD development (Fig. 3E).

The expression profile of METTL3 and WTAP is closely associated with the deposition of Aβ

m6A modification is catalyzed by the m6A methyltransferase complex, which consists of METTL3, METTL14, and WTAP. Among them, METTL3 is the core component of the m6A methyltransferase complex and plays a catalytic role, which is responsible for the catalytic activity of the complex, transferring the methyl group from S-adenosylmethionine (SAM) to the target RNA molecule [30]. Specifically, WTAP functions as a regulatory factor in the complex, modulating the localization and activity of the complex to promote efficient m6A modification [7]. Previous studies have demonstrated that the expression of WTAP and METTL3 is dysregulated in the brains of AD patients and in animal models of AD [22]. In the aforementioned RT-qPCR experiment, we observed a significant downregulation of *Mettl3* and *Wtap* in the hippocampal region of 5xFAD mice as early as 3-month-old. This suggested the potential involvement of m6A regulatory factors in the onset of AD. To further validate this findings, we examined the expression profile of these proteins in the hippocampus during AD progression. The analysis of the fluorescence intensity showed no significant difference in the expression of METTL3 and WTAP in the AD group compared to the WT group at 1-month age (sFig. 7). The expression of WTAP and METTL3 surrounding the Aβ exhibited a decrease in abundance only after the appearance of significant Aβ accumulation (Fig. 4). The reduction of WTAP began as early as 3 months old, whereas the decrease in METTL3 expression started close to 6 months old. This implies that the decline in METTL3 expression occurs earlier than WTAP during the development of AD (Fig. 4E and 4K).

MeRIP-seq analysis of AD brain

To gain a deeper understanding of RNA m6A modification changes in AD, Methylated RNA Immunoprecipitation Sequencing (MeRIP-seq) was performed on the whole brain of 9-month-old 5xFAD and age-matched C57BL/6 control mice, with four mice in each group. MeRIP-seq results were analyzed, and m6A peaks with |fold change|>1.5 and $P < 0.05$ were selected for both the WT and 5xFAD groups, peaks represented regions in the genome that are modified with m6A. The results showed that there were 11,664 and 11,573 m6A modification sites in the WT and 5xFAD groups, respectively, with 10,884 overlapping m6A modification sites between the two groups (Fig. 5C, supplementary table2). The exomePeak package was used for genome-wide peak scanning, and it was found that m6A peaks were mainly distributed in the coding region (CDS), 3' untranslated region (3'UTR), and 5' untranslated region (5'UTR) in both the AD and WT control groups (sFig. 5B). The differential peaks between the two groups were then analyzed, and it was found that, compared to the WT group, the 5xFAD group had 607 upregulated and 645 downregulated m6A peaks (Fig. 5D). The Gene Ontology (GO) and Kyoto Encyclopedia of Genes and Genomes (KEGG) annotations suggested that differentially expressed m6A-modified genes found in 5xFAD were involved in DNA damage, cellular senescence, apoptosis, and N-glycan biosynthesis (Fig. 5E and 5F, and supplementary table 3).

To investigate the relationship between m6A methylation and gene expression in the AD process, we performed RNA sequencing (RNA-seq) on brain tissues from 5xFAD and WT mice. The analysis of

differentially expressed genes (DEGs) showed that, compared to the WT group, 77 genes were significantly upregulated and 31 genes were significantly downregulated in the 5xFAD group (Fig. 6A). Subsequently, based on the results of differential genes and differential peaks, a correlation analysis was performed to integrate transcription with m6A methylation levels (Fig. 6B). A four-quadrant plot was generated to observe changes in gene expression as m6A methylation levels changed. The Hyper-up quadrant represents upregulated m6A peaks and upregulated gene expression; the Hyper-down quadrant represents upregulated m6A peaks and downregulated gene expression; the Hypo-up quadrant represents downregulated m6A peaks and upregulated gene expression; and the Hypo-down quadrant represents downregulated m6A peaks and downregulated gene expression. We identified 25 genes in the hyper-up quadrant (like *Clec7a*, *Mpeg1*, *H2q7*, *H2k1*), 14 genes in the hypo-down quadrant (*Pigh*, *Tomt, Zbed5*), 33 genes in the hyper-down quadrant (*Cap6*, *Cstad*, *Lsm2, Cradd*) and 31 genes in the hypo-up quadrant (*Ilr1*, *Gvin1*, *Ch25h*, *Ifit3*) (Fig. 6B and supplementary table 4).

Next, we performed GO term enrichment and KEGG analysis on the genes identified in the four quadrants. The results showed that the genes with differential m6A peaks identified in the AD were enriched in processes such as regulation of IFNγ production, VEGF production, and regulation of Th1 immune response (Fig. 6C). These are crucial for immune system function [31–33].The KEGG analysis revealed that the genes with expression related to m6A peak changes in the AD group were mainly enriched in several pathways, including neutrophil extracellular trap formation, cytokine-cytokine receptor interaction, steroid hormone biosynthesis, platelet activation, primary bile acid biosynthesis, and glycosaminoglycan degradation (Fig. 6D and supplementary table 5). These pathways have been implicated in the clearance of Aβ plaques, regulation of innate immune response, regulation of neuroprotective, regulation of cerebral blood flow and lipid metabolism in the brain, respectively [34–37].

mRNA m6A methylation and the correlation with microglia transcription

Based on the annotation in the differential peaks identified in m6A-seq data, there may be a connection between mRNA m6A methylation and the regulation of microglial gene expression, which is relevant to the pathogenesis of AD. Indeed, microglia are crucial for AD development, and disease-associated microglia (DAM) are a specific subset of microglia that have been identified in the context of neurodegenerative diseases such as AD. We observed 25 DAM genes were highly expressed in 9-month-old AD brains. (Fig. 7Aand 7B). In these 25 genes, most of them exhibit increased m6A modifications, such as *Csf1*, *Cd*6, *Mpge1*, and *Cd68* (Fig. 7D). These studies propose a link between m6A modifications and the function of microglia in AD. Thus, we employed the MACS technique to isolate microglia from 9-month-old AD mice and examined the expression of m6A and m6A enzymes (Fig. 7E). Our findings revealed an upward trend in m6A levels within microglia (Fig. 7F). Notably, m6A writers *Ythdf1*, *Ythdf2*, *Ythdf3*, and the eraser *Alkbh5* exhibited a significant upregulation (Fig. 7G). We further observed upregulated expression of ALKBH5 but not m6A writers in microglia surrounding Aβ plaques within the hippocampal region (Fig. 7H), suggesting the implication of ALKBH5 in microglial response to Aβ plaques accumulation.

Discussion

mRNA m6A methylation has been found to be associated with the occurrence of cancer, such as breast cancer and lung cancer [38], but the relationship between RNA m6A methylation and the central nervous system is largely unknown. Although the level of mRNA m6A modification is relatively high in the brain, research on m6A-modified RNA in the brain is still a nascent field, and the significance of this epigenetic marker in the CNS has only recently been recognized [23, 39]. In this study, we focused on investigating the dynamic changes in mRNA m6A and m6A enzymes during the development of AD. Immunofluorescence staining revealed that RNA m6A modification is relatively high in neurons, but low in glial cells. But the precise reason for the low level of m6A expression in glial cells compared to neurons is not yet fully understood. The overall level of m6A modification gradually decreases with age, but there was no significant difference detected in total m6A levels between AD and normal controls at the same age. However, after detecting Aβ accumulation at 3 months of age, we observed a decrease in m6A levels surrounding Aβ plaques. Furthermore, we observed changes in the expression of m6A enzymes during AD development, with downregulation of METTL3 and WTAP occurring as early as 3 months of age, suggesting a link between dysregulated m6A RNA modification and the onset of AD.

Similarly, a previous study analyzed a public RNA-seq dataset and found that the RNA methyltransferase METTL3 and the component of the m6A methyltransferase complex RBM15B were downregulated and upregulated, respectively, in the hippocampus [40]. Additionally, our finding is consistent with other studies that demonstrated decreased levels of METTL3 and METTL14 in the brain tissue from patients with mild cognitive impairment, a precursor stage of AD, suggesting a potential role for mRNA m6A modification in the early stages of the disease [22]. In adult mouse hippocampus, the reduction of m6A modification caused by *Mettl3* gene knockout resulted in cognitive and memory impairment, which are characteristic manifestations of AD. This study also demonstrated that METTL3 is necessary for the maintenance of dendritic spine and synaptic integrity, as well as neuronal survival. Another study showed that suppression of FTO demethylase to restore m6A modification levels in an AD model rescued pathological changes in the brain, such as neuronal death. However, in contrast to our finding, another study found that the level of mRNA m6A methylation is increased in the cortex and hippocampus of an AD mouse model (APP/PS1 transgenic mice) compared to control, and the expression level of METTL3 is upregulated while FTO is downregulated in AD mice [41]. The reason for this discrepancy may be attributed to the different AD mouse models used.

Lastly, analysis of m6A-seq in the brains of AD and WT mice, we found that the differentially methylated peaks were enriched in GO and KEGG terms related to processes such as inflammation response, immune system processes, signal transduction, positive regulation of lipid metabolism, and cytokine production. These findings suggest a link between mRNA m6A methylation and the regulation of microglia gene expression. Microglia are immune cells that play a critical role in the central nervous system, and dysregulation of microglial activation has been implicated in the pathogenesis of neurodegenerative diseases, including AD [42]. One study found that silencing of the m6A methyltransferase METTL14

resulted in decreased expression of pro-inflammatory genes and increased expression of anti-inflammatory genes in microglia, suggesting that m6A methylation regulates microglial polarization and activation [43]. Another study found that the m6A methyltransferase METTL3 was upregulated in activated microglia in response to lipopolysaccharide (LPS) stimulation. Inhibition of METTL3 resulted in decreased expression of pro-inflammatory cytokines and chemokines in microglia, indicating that m6A methylation is involved in the regulation of microglial inflammatory responses [44]. In addition, a recent study found that m6A methylation plays a critical role in the regulation of microglial phagocytosis [45]. Our observation suggested ALKBH5 is close like to microglia response to Aβ accumulation. Taken together, these findings suggest that mRNA m6A methylation plays a crucial role in the regulation of microglia function and gene expression, and dysregulation of this process may contribute to the pathogenesis of neurodegenerative diseases such as AD.

Declarations

Ethics approval and consent to participate

All animal procedures adhered to the guidelines set by the Institutional Animal Care and Use Committee and were conducted in the Animal Facility of the Department of Laboratory Animal Science at Fudan University.

Consent for publication

Not applicable.

Availability of data and materials

MeRIP-seq data are available in the Genome Sequence Archive (GSA) with accession code CRA010646.

Competing interests

The authors have no conflicts of interest to disclose. All authors grant permission to publish the submitted content.

Funding

This work was supported by grants from the National Natural Science Foundation of China (32170958).

Author contributions

Y.R. and B.P. conceived and designed this study. Y.R. and B.P supervised and conceptualized this study. Y.R., and Y.W. wrote the manuscript. Y.W. performed most experiments. X.L. analyzed the sequencing results, J.W.,T.-F.Y. provided necessary study support. All authors discussed the results and commented on this manuscript.

Acknowledgements

The authors thank Yuxiao Jin, Shuai Gao (Fudan University) for donating 5xFAD mice. Fang Lei and Jiachen Zhu (Fudan University) for the excellent laboratory management. Yanxia Rao would like to express her gratitude to Pai Peng for his patience and support during the drafting of this manuscript. In addition, the authors express their gratitude and respect to all animals sacrificed in this study. In memory of Prof. Huaxi Xu. This study was supported by STI2030-Major Projects (2022ZD0207200) (Y.R.) and (2022ZD0204700) (B.P.), National Natural Science Foundation of China (32170958) (B.P.), Program of Shanghai Academic/Technology Research Leader (21XD1420400) (B.P.), Shanghai Pilot Program for Basic Research (21TQ014) (B.P.), The Innovative Research Team of High-Level Local University in Shanghai (B.P.).

References

1. Larson EB, Kukull WA, Katzman RL. Cognitive impairment: dementia and Alzheimer's disease. Annual review of public health. 1992; **13:** 431-49. http://dx.doi.org/10.1146/annurev.pu.13.050192.002243.
2. Scheltens P, De Strooper B, Kivipelto M, Holstege H, Chételat G, Teunissen CE, et al. Alzheimer's disease. Lancet. 2021; **397:** 1577-1590. http://dx.doi.org/10.1016/S0140-6736(20)32205-4.
3. Xu W, Tan L, Wang HF, Jiang T, Tan MS, Tan L, et al. Meta-analysis of modifiable risk factors for Alzheimer's disease. Journal of neurology, neurosurgery, and psychiatry. 2015; **86:** 1299-306. http://dx.doi.org/10.1136/jnnp-2015-310548.
4. Fu Y, Dominissini D, Rechavi G, He C. Gene expression regulation mediated through reversible m A RNA methylation. Nature reviews. Genetics. 2014; **15:** 293-306. http://dx.doi.org/10.1038/nrg3724.
5. Jiang X, Liu B, Nie Z, Duan L, Xiong Q, Jin Z, et al. The role of m6A modification in the biological functions and diseases. Signal transduction and targeted therapy. 2021; **6:** 74. http://dx.doi.org/10.1038/s41392-020-00450-x.
6. Liu J, Yue Y, Han D, Wang X, Fu Y, Zhang L, et al. A METTL3-METTL14 complex mediates mammalian nuclear RNA N6-adenosine methylation. Nat Chem Biol. 2014; **10:** 93-5. http://dx.doi.org/10.1038/nchembio.1432.
7. Ping XL, Sun BF, Wang L, Xiao W, Yang X, Wang WJ, et al. Mammalian WTAP is a regulatory subunit of the RNA N6-methyladenosine methyltransferase. Cell Res. 2014; **24:** 177-89. http://dx.doi.org/10.1038/cr.2014.3.
8. Jia G, Fu Y, Zhao X, Dai Q, Zheng G, Yang Y, et al. N6-methyladenosine in nuclear RNA is a major substrate of the obesity-associated FTO. Nat Chem Biol. 2011; **7:** 885-7. http://dx.doi.org/10.1038/nchembio.687.
9. Tang C, Klukovich R, Peng H, Wang Z, Yu T, Zhang Y, et al. ALKBH5-dependent m6A demethylation controls splicing and stability of long 3'-UTR mRNAs in male germ cells. Proceedings of the National Academy of Sciences of the United States of America. 2018; **115:** E325-e333. http://dx.doi.org/10.1073/pnas.1717794115.

10. Liu N, Dai Q, Zheng G, He C, Parisien M, Pan T. N(6)-methyladenosine-dependent RNA structural switches regulate RNA-protein interactions. Nature. 2015; **518:** 560-4. http://dx.doi.org/10.1038/nature14234.
11. Wu B, Su S, Patil DP, Liu H, Gan J, Jaffrey SR, et al. Molecular basis for the specific and multivariant recognitions of RNA substrates by human hnRNP A2/B1. Nature communications. 2018; **9:** 420. http://dx.doi.org/10.1038/s41467-017-02770-z.
12. Meyer KD, Patil DP, Zhou J, Zinoviev A, Skabkin MA, Elemento O, et al. 5' UTR m(6)A Promotes Cap-Independent Translation. Cell. 2015; **163:** 999-1010. http://dx.doi.org/10.1016/j.cell.2015.10.012.
13. Miao Z, Zhang T, Qi Y, Song J, Han Z, Ma C. Evolution of the RNA N (6)-Methyladenosine Methylome Mediated by Genomic Duplication. Plant Physiol. 2020; **182:** 345-360. http://dx.doi.org/10.1104/pp.19.00323.
14. Bale TL. Epigenetic and transgenerational reprogramming of brain development. Nature reviews. Neuroscience. 2015; **16:** 332-44. http://dx.doi.org/10.1038/nrn3818.
15. Huang AZ, Delaidelli A, Sorensen PH. RNA modifications in brain tumorigenesis. Acta neuropathologica communications. 2020; **8:** 64. http://dx.doi.org/10.1186/s40478-020-00941-6.
16. Shafik AM, Zhang F, Guo Z, Dai Q, Pajdzik K, Li Y, et al. N6-methyladenosine dynamics in neurodevelopment and aging, and its potential role in Alzheimer's disease. Genome Biol. 2021; **22:** 17. http://dx.doi.org/10.1186/s13059-020-02249-z.
17. Armstrong MJ, Jin Y, Allen EG, Jin P. Diverse and dynamic DNA modifications in brain and diseases. Human molecular genetics. 2019; **28:** R241-r253. http://dx.doi.org/10.1093/hmg/ddz179.
18. Shi H, Zhang X, Weng YL, Lu Z, Liu Y, Lu Z, et al. m(6)A facilitates hippocampus-dependent learning and memory through YTHDF1. Nature. 2018; **563:** 249-253. http://dx.doi.org/10.1038/s41586-018-0666-1.
19. Du T, Li G, Yang J, Ma K. RNA demethylase Alkbh5 is widely expressed in neurons and decreased during brain development. Brain research bulletin. 2020; **163:** 150-159. http://dx.doi.org/10.1016/j.brainresbull.2020.07.018.
20. Yen YP, Chen JA. The m(6)A epitranscriptome on neural development and degeneration. Journal of biomedical science. 2021; **28:** 40. http://dx.doi.org/10.1186/s12929-021-00734-6.
21. Zhang R, Zhang Y, Guo F, Li S, Cui H. RNA N6-Methyladenosine Modifications and Its Roles in Alzheimer's Disease. Frontiers in cellular neuroscience. 2022; **16:** 820378. http://dx.doi.org/10.3389/fncel.2022.820378.
22. Zhao F, Xu Y, Gao S, Qin L, Austria Q, Siedlak SL, et al. METTL3-dependent RNA m(6)A dysregulation contributes to neurodegeneration in Alzheimer's disease through aberrant cell cycle events. Mol Neurodegener. 2021; **16:** 70. http://dx.doi.org/10.1186/s13024-021-00484-x.
23. Widagdo J, Zhao QY, Kempen MJ, Tan MC, Ratnu VS, Wei W, et al. Experience-Dependent Accumulation of N6-Methyladenosine in the Prefrontal Cortex Is Associated with Memory Processes in Mice. The Journal of neuroscience : the official journal of the Society for Neuroscience. 2016; **36:** 6771-7. http://dx.doi.org/10.1523/jneurosci.4053-15.2016.

24. Jawhar S, Trawicka A, Jenneckens C, Bayer TA, Wirths O. Motor deficits, neuron loss, and reduced anxiety coinciding with axonal degeneration and intraneuronal Aβ aggregation in the 5XFAD mouse model of Alzheimer's disease. Neurobiology of aging. 2012; **33:** 196.e29-40. http://dx.doi.org/10.1016/j.neurobiolaging.2010.05.027.
25. Li R, Zhang C, Rao Y, Yuan T-F. Deep brain stimulation of fornix for memory improvement in Alzheimer's disease: A critical review. Ageing Research Reviews. 2022; **79:** http://dx.doi.org/10.1016/j.arr.2022.101668.
26. Guerreiro R, Wojtas A, Bras J, Carrasquillo M, Rogaeva E, Majounie EJNEJM. TREM2 variants in Alzheimer's disease. 2013; **368:** http://dx.doi.org/10.1056/NEJMoa1211851.
27. Forner S, Kawauchi S, Balderrama-Gutierrez G, Kramár EA, Matheos DP, Phan J, et al. Systematic phenotyping and characterization of the 5xFAD mouse model of Alzheimer's disease. Scientific data. 2021; **8:** 270. http://dx.doi.org/10.1038/s41597-021-01054-y.
28. Zhuang M, Geng X, Han P, Che P, Liang F, Liu C, et al. YTHDF2 in dentate gyrus is the m(6)A reader mediating m(6)A modification in hippocampus-dependent learning and memory. Mol Psychiatry. 2023; http://dx.doi.org/10.1038/s41380-023-01953-z.
29. Martinez De La Cruz B, Gell C, Markus R, Macdonald I, Fray R, Knight HM. m(6) A mRNA methylation in human brain is disrupted in Lewy body disorders. Neuropathology and applied neurobiology. 2023; **49:** e12885. http://dx.doi.org/10.1111/nan.12885.
30. Wang P, Doxtader KA, Nam Y. Structural Basis for Cooperative Function of Mettl3 and Mettl14 Methyltransferases. Molecular cell. 2016; **63:** 306-317. http://dx.doi.org/10.1016/j.molcel.2016.05.041.
31. Gocher AM, Workman CJ, Vignali DAA. Interferon-γ: teammate or opponent in the tumour microenvironment? Nature reviews. Immunology. 2022; **22:** 158-172. http://dx.doi.org/10.1038/s41577-021-00566-3.
32. Apte RS, Chen DS, Ferrara N. VEGF in Signaling and Disease: Beyond Discovery and Development. Cell. 2019; **176:** 1248-1264. http://dx.doi.org/10.1016/j.cell.2019.01.021.
33. Geremia A, Biancheri P, Allan P, Corazza GR, Di Sabatino A. Innate and adaptive immunity in inflammatory bowel disease. Autoimmunity reviews. 2014; **13:** 3-10. http://dx.doi.org/10.1016/j.autrev.2013.06.004.
34. Zenaro E, Pietronigro E, Della Bianca V, Piacentino G, Marongiu L, Budui S, et al. Neutrophils promote Alzheimer's disease-like pathology and cognitive decline via LFA-1 integrin. Nature medicine. 2015; **21:** 880-6. http://dx.doi.org/10.1038/nm.3913.
35. Thurlow JK, Peña Murillo CL, Hunter KD, Buffa FM, Patiar S, Betts G, et al. Spectral clustering of microarray data elucidates the roles of microenvironment remodeling and immune responses in survival of head and neck squamous cell carcinoma. Journal of clinical oncology : official journal of the American Society of Clinical Oncology. 2010; **28:** 2881-8. http://dx.doi.org/10.1200/jco.2009.24.8724.

36. Schumacher M, Weill-Engerer S, Liere P, Robert F, Franklin RJ, Garcia-Segura LM, et al. Steroid hormones and neurosteroids in normal and pathological aging of the nervous system. Progress in neurobiology. 2003; **71:** 3-29. http://dx.doi.org/10.1016/j.pneurobio.2003.09.004.
37. Grande-Allen KJ, Osman N, Ballinger ML, Dadlani H, Marasco S, Little PJ. Glycosaminoglycan synthesis and structure as targets for the prevention of calcific aortic valve disease. Cardiovascular research. 2007; **76:** 19-28. http://dx.doi.org/10.1016/j.cardiores.2007.05.014.
38. Kaklamani V, Yi N, Sadim M, Siziopikou K, Zhang K, Xu Y, et al. The role of the fat mass and obesity associated gene (FTO) in breast cancer risk. BMC medical genetics. 2011; **12:** 52. http://dx.doi.org/10.1186/1471-2350-12-52.
39. Meyer KD, Saletore Y, Zumbo P, Elemento O, Mason CE, Jaffrey SR. Comprehensive analysis of mRNA methylation reveals enrichment in 3' UTRs and near stop codons. Cell. 2012; **149:** 1635-46. http://dx.doi.org/10.1016/j.cell.2012.05.003.
40. Huang H, Camats-Perna J, Medeiros R, Anggono V, Widagdo J. Altered Expression of the m6A Methyltransferase METTL3 in Alzheimer's Disease. eNeuro. 2020; **7:** http://dx.doi.org/10.1523/eneuro.0125-20.2020.
41. Han M, Liu Z, Xu Y, Liu X, Wang D, Li F, et al. Abnormality of m6A mRNA Methylation Is Involved in Alzheimer's Disease. Front Neurosci. 2020; **14:** 98. http://dx.doi.org/10.3389/fnins.2020.00098.
42. Varnum MM, Ikezu T. The classification of microglial activation phenotypes on neurodegeneration and regeneration in Alzheimer's disease brain. Archivum immunologiae et therapiae experimentalis. 2012; **60:** 251-66. http://dx.doi.org/10.1007/s00005-012-0181-2.
43. Du J, Liao W, Liu W, Deb DK, He L, Hsu PJ, et al. N(6)-Adenosine Methylation of Socs1 mRNA Is Required to Sustain the Negative Feedback Control of Macrophage Activation. Developmental cell. 2020; **55:** 737-753.e7. http://dx.doi.org/10.1016/j.devcel.2020.10.023.
44. Wen L, Sun W, Xia D, Wang Y, Li J, Yang S. The m6A methyltransferase METTL3 promotes LPS-induced microglia inflammation through TRAF6/NF-κB pathway. Neuroreport. 2022; **33:** 243-251. http://dx.doi.org/10.1097/wnr.0000000000001550.
45. You S, Su X, Ying J, Li S, Qu Y, Mu D. Research Progress on the Role of RNA m6A Modification in Glial Cells in the Regulation of Neurological Diseases. Biomolecules. 2022; **12:** http://dx.doi.org/10.3390/biom12081158.
46. Minhas PS, Latif-Hernandez A, McReynolds MR, Durairaj AS, Wang Q, Rubin A, et al. Restoring metabolism of myeloid cells reverses cognitive decline in ageing. Nature. 2021; **590:** 122-128. http://dx.doi.org/10.1038/s41586-020-03160-0.

Figures

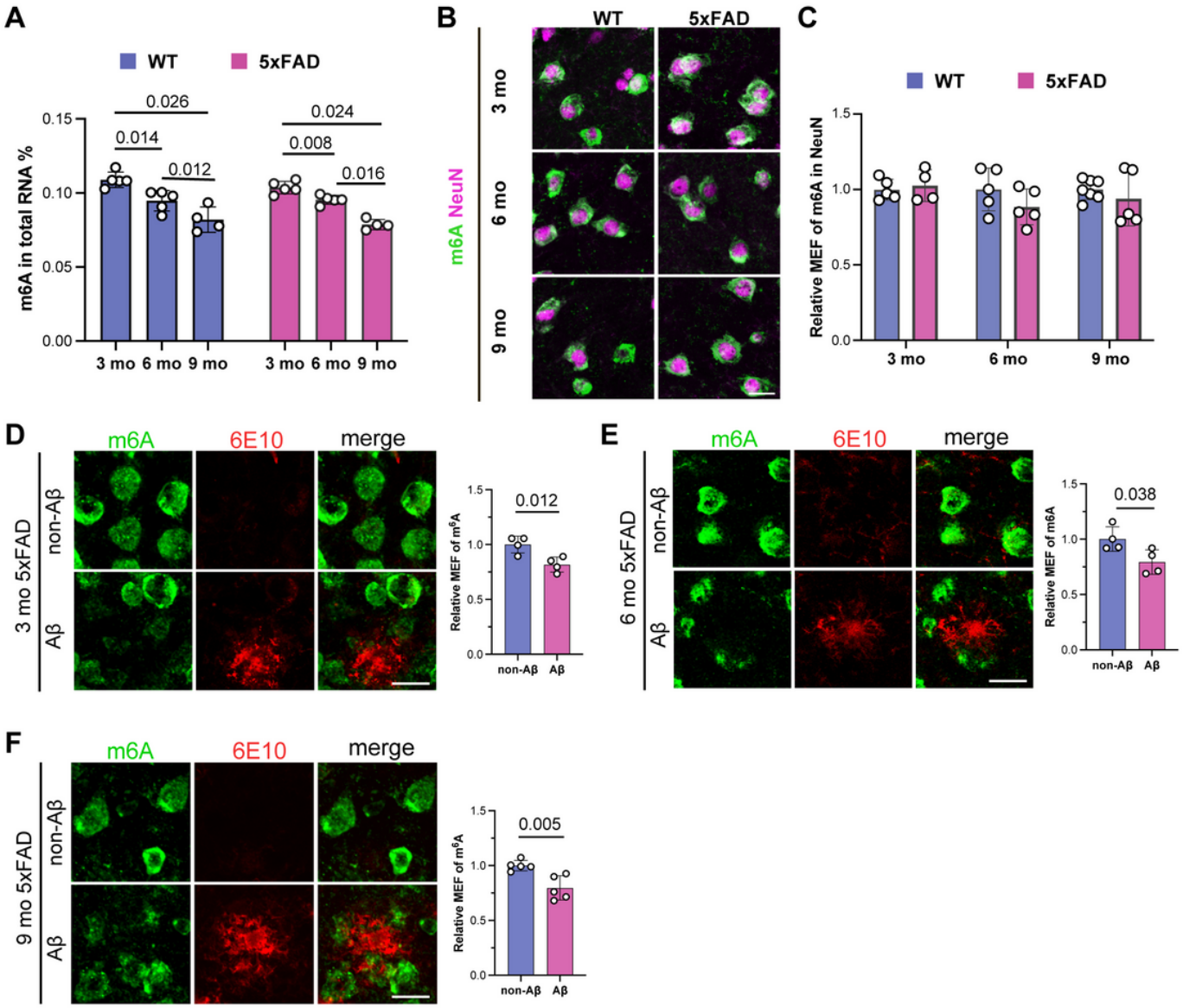

Figure 1

Age-related changes in m6A levels in nomral and 5xFAD. (**A**) The quantitative of m6A methylation in the hippocampus of 3, 6 and 9-month-old mice showed a significant decrease in m6A levels as the mice aged. (**B**) Co-staining of m6A and neuron marker NeuN in hippocampus of 5xFAD and age-matched WT mice. (**C**) Colocalization analysis of m6A with NeuN in hippocampal of 3, 6 and 9-momth-old 5xFAD and WT mice brains. (**D-F**) Representaive images showing m6A expression around Aβ and non-Aβ regions in the brain of 3, 6 and 9-month-old 5xFAD mice. Data were presented as mean ± SD. Scale bar is 20 μm.

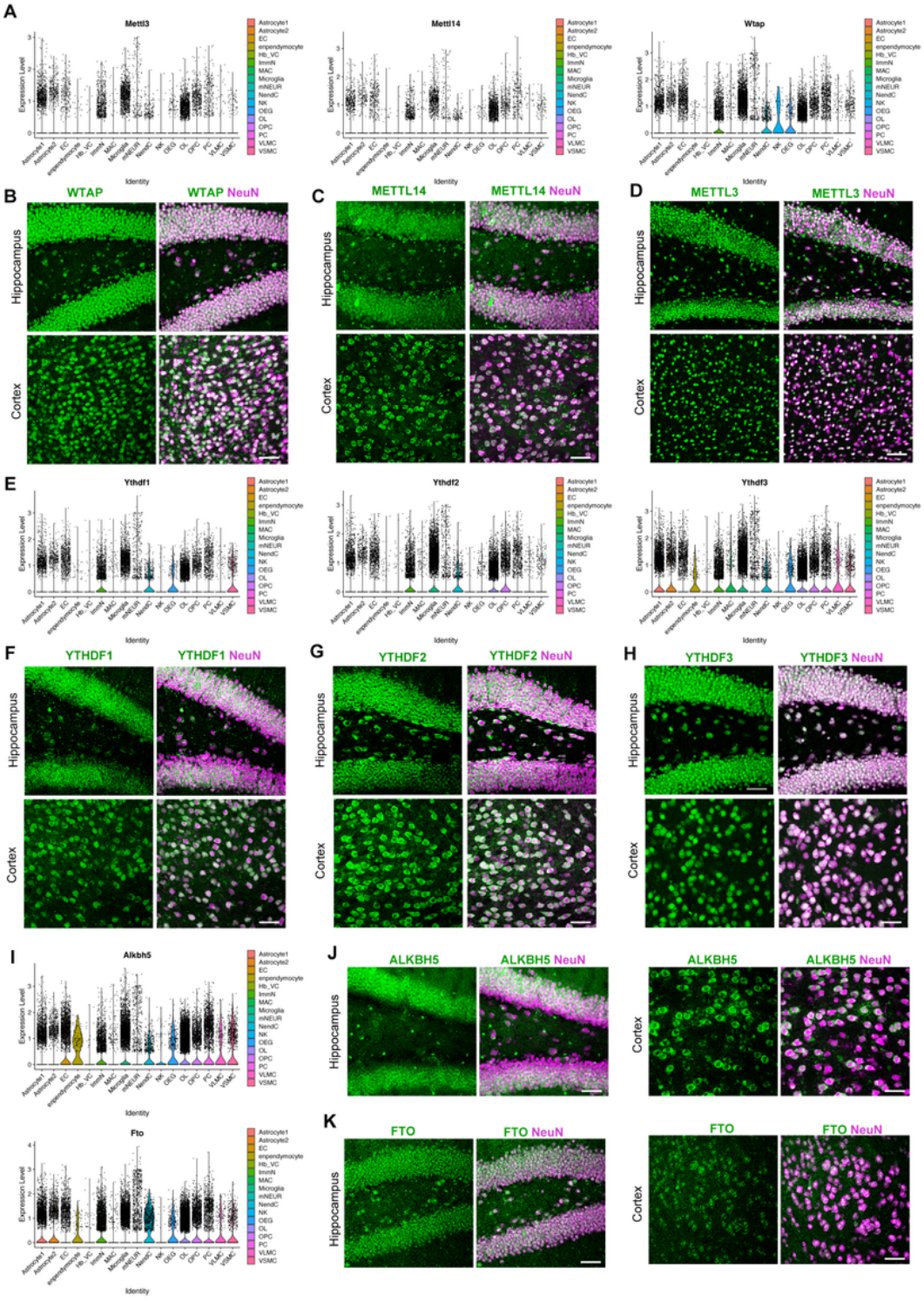

Figure 2

Cellular localization of m6A-related genes in mouse brain. (**A**) scRNA-seq data from the whole brain showing the relative expression of m6A "writers" (METTL3/14, WTAP) in neurons and glial cells of adult normal mice. (**B-D**) Double labeling of adult WT mouse brains (3-months of age) with m6A "writers" (METTL3/14, WTAP) and NeuN antibodies in the hippocampus and cerebral cortex. (**E**) scRNA-seq results showing the expression patterns of m6A "readers" (YTHDF1-3). [46] Co-expression of m6A "readers"

(YTHDF1-3) and NeuN in mouse hippocampal and cortex tissues. (**I**) scRNA-seq results showing the expression patterns of m6A “erasers” (ALKBH5, FTO). (**J, K**) Representative confocal images showing the co-staining of ALKBH5 and FTO with NeuN, respectively. Scale bar is 50 μm.

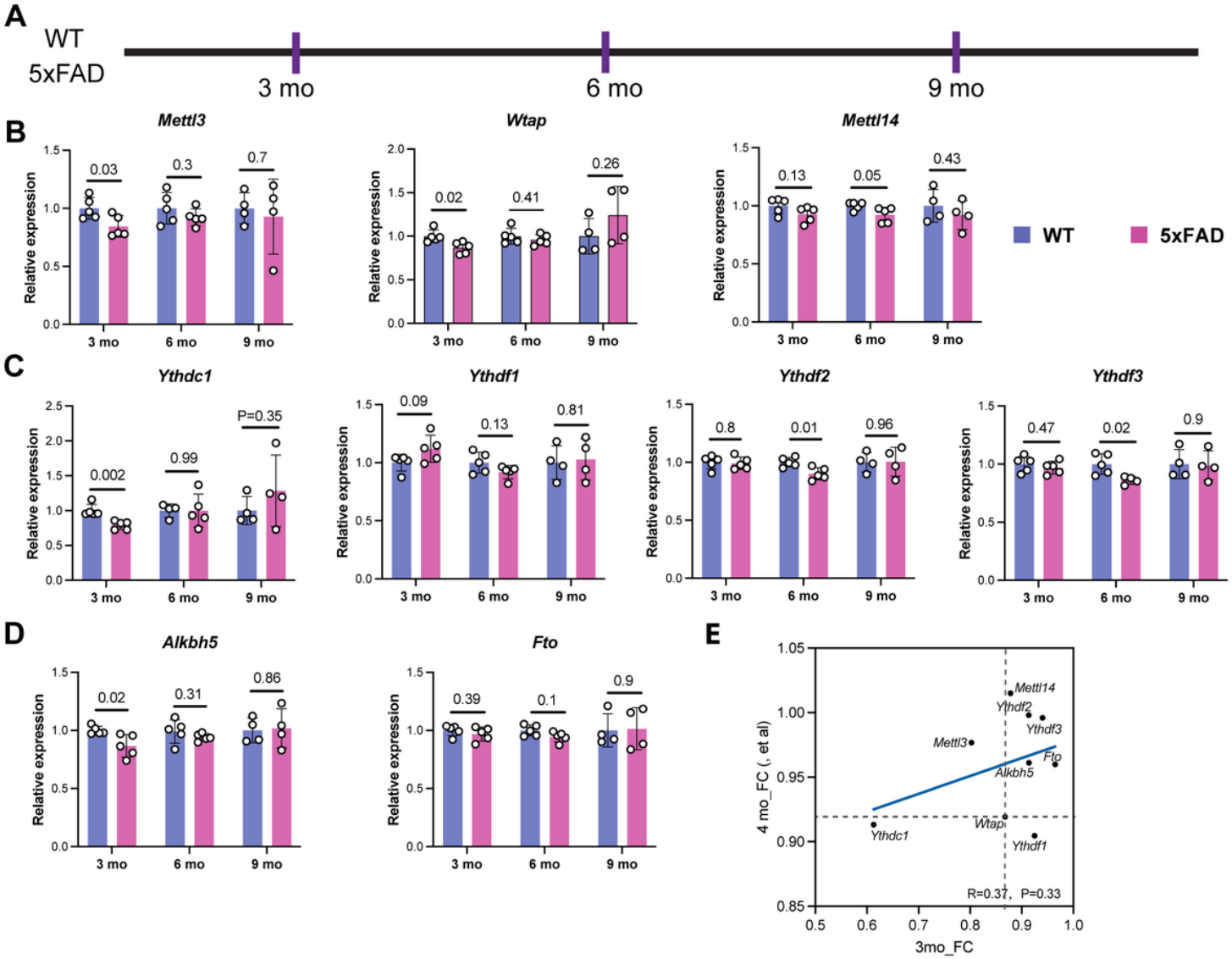

Figure 3

Dynamic expression of m6A regulatory factors in the progression of AD. (**A**) Scheme showing the expriment design and time point for RT-qPCR. (3, 6 and 9-months of age). (**B-D)** Quantification of relative expression level of m6A-related genes. N=5 biological replicates for WT and 5xFAD group. Two-tailed independent t test, p< 0.05. p value are provided in the figures. (**E**) Correlation analysis was performed using the fold change of the m6A-ralated genes between 3 and 4-month-old mice from public data (GSE168137).

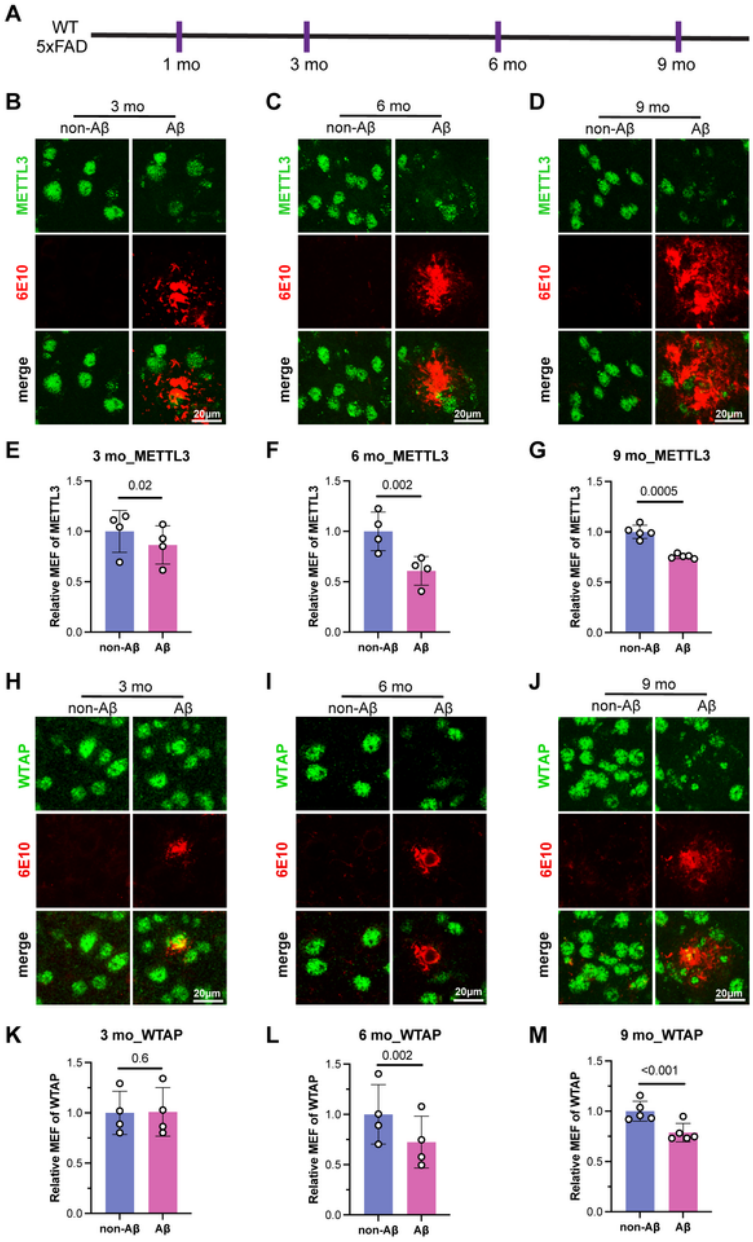

Figure 4

The presence of amyloid-beta (Aβ) pathology affects the expression levels of METTL3 and WTAP. (**A**) Scheme showing the experiment design and time point for examination. (**B-D**) Representative confocal images showing the expression of METTL3 and 6E10 (Aβ). (**E-G**) Statistics of the fluorescence intensity of METTL3 around Aβ and non-Aβ regions in 3, 6 and 9-month-old 5xFAD mice brains. N=4 or 5 mice for each group. Two-tailed independent t test, $p<0.05$. (**H-J**) Representative confocal images of co-staining of

WTAP and 6E10 (Aβ). (**K-M**) Statistics of the fluorescence intensity of WTAP around Aβ and non-Aβ regions in 3, 6 and 9-month-old 5xFAD mice brains. N=4 or 5 mice for each group. Two-tailed independent t test. Scale bar is 20 μm.

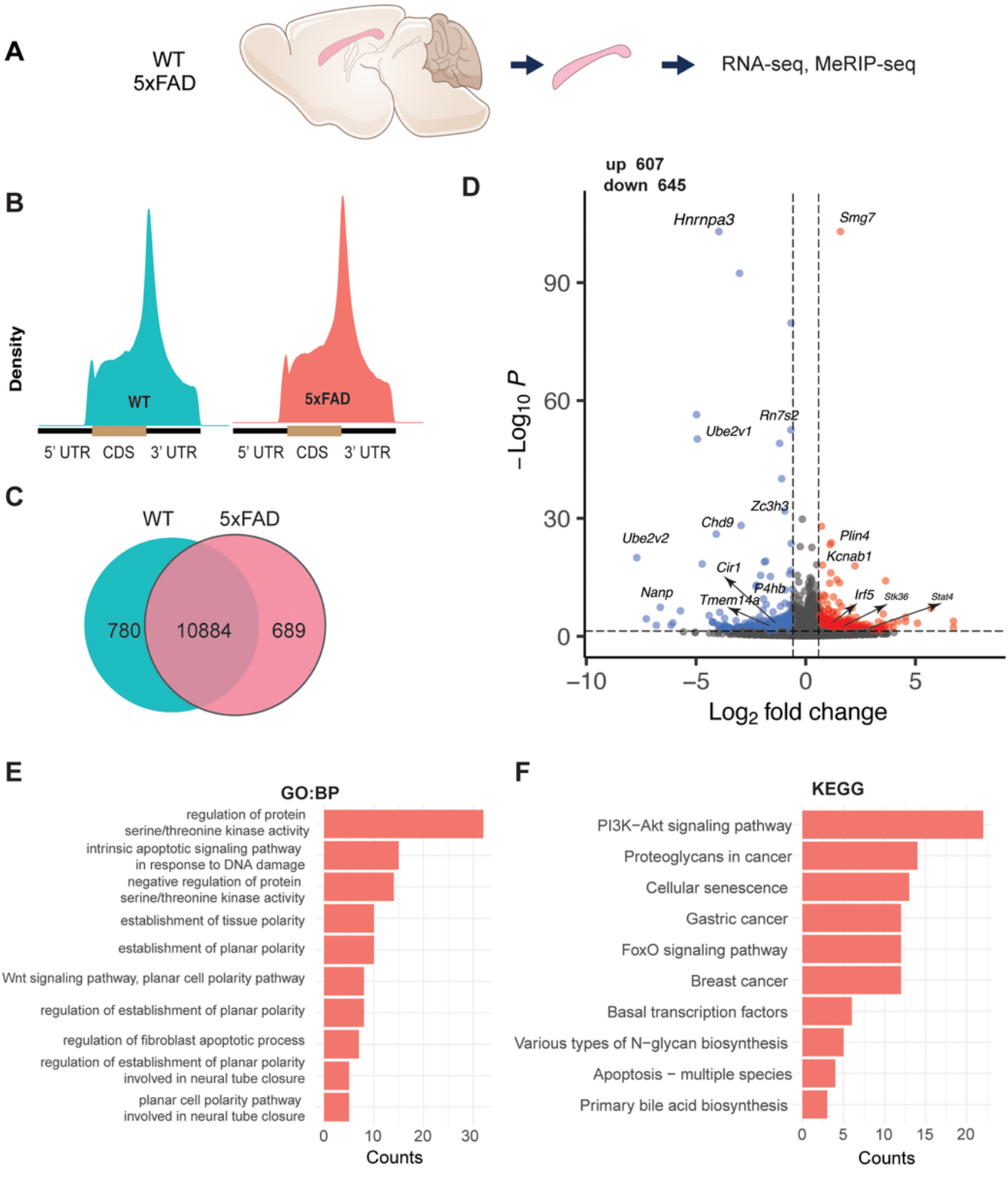

Figure 5

MeRIP-seq domenstrates the alteration in the m6A modification patterns in 5xFAD (**A**) Schematic diagram representation of MeRIP-seq. (**B**) Distribition of the region of the average m6A peaks regions across all transcripts in WT and 5xFAD. (**C**) Venn diagram showing the identified m6A peaks in WT and 5xFAD. (**D**) Volcano plots showing mRNAs with significantly altered m6A peaks in 5xFAD. (**E**) The top 10 GO terms with the greatest number of enriched genes. (**F**) The top 10 KEGG pathways with the greatest number of enriched genes.

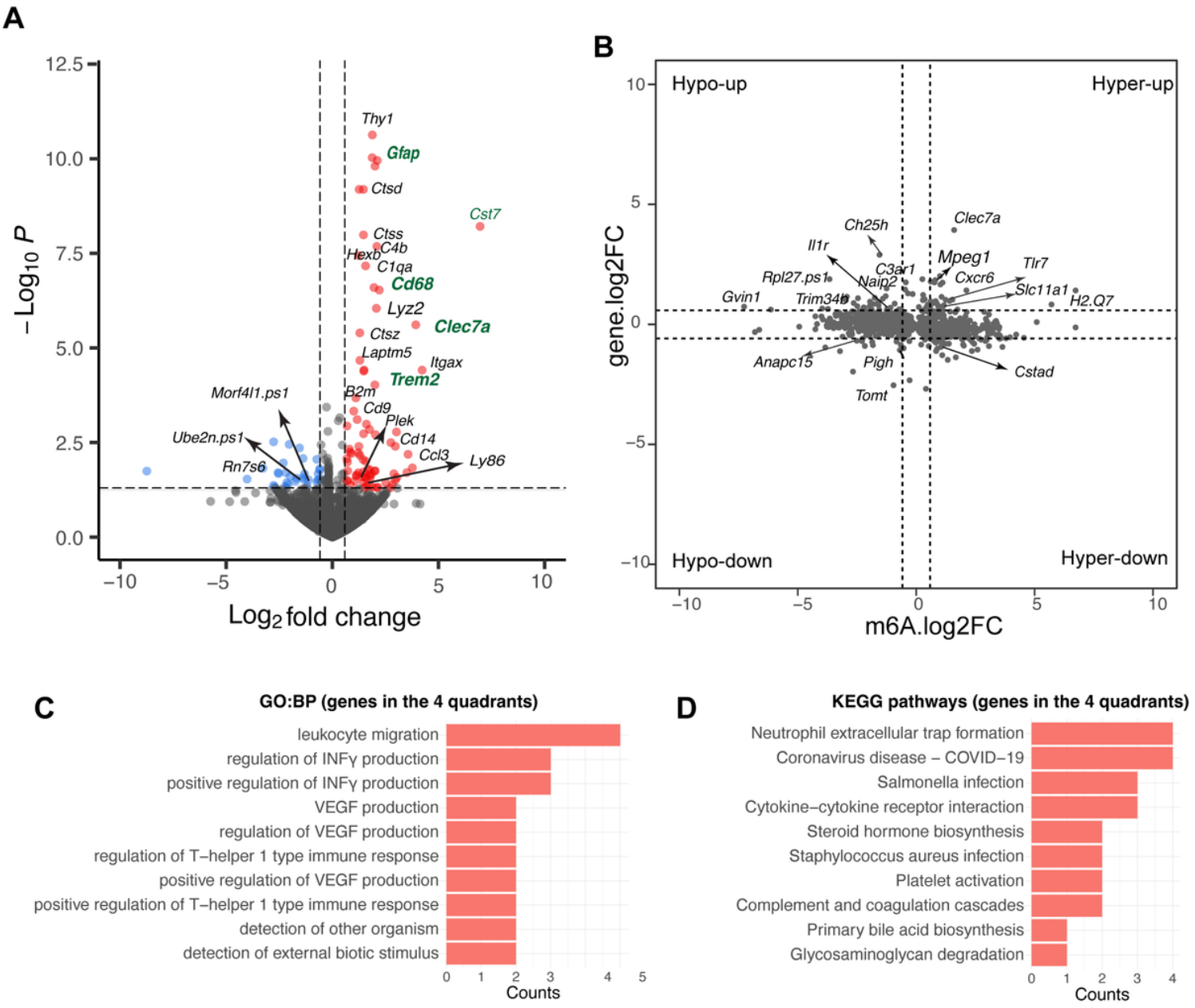

Figure 6

Correlation analysis of differential genes and differential peaks . (**A**) Volcano plots showing the differentially expressed genes in 5xFAD. (**B**) Four-quadrant plots showing the distribution of genes with altered m6A modification and mRNA levels. (**C**) The top 10 GO terms with the greatest number of enriched genes. (**D**) The top 10 KEGG pathways with the greatest number of enriched genes.

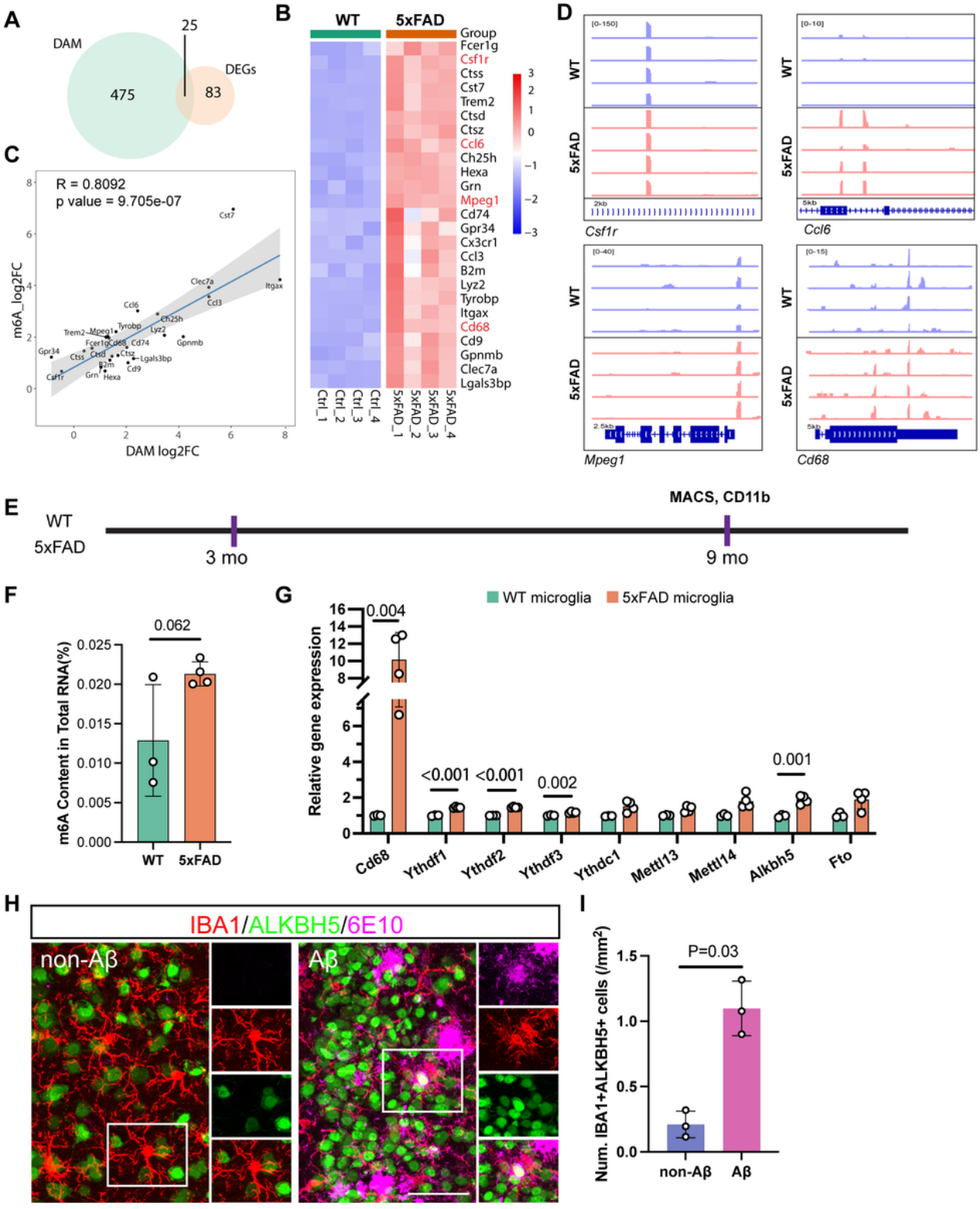

Figure 7

Genes with altered m6A modification pattern are associated to microglia in 5xFAD mice. (**A**) Venn diagrams for genes with either disease-associated microglia (DAM) and differentially expressed genes (DEGs). (**B**) Heatmap showing the expression of 25 DAM genes in 9-month-old AD brains. (**C**) Correlation analysis betwwen DAM and DEGs identified in 9-month old AD brains. (**D**) *Csf1*, *Ccl6*, *Mpeg1* and *Cd68* exhibit increased m6A modifications in AD brains. (**E**) Scheme showing the method for MACS to isolate

microglia from 9-month-old AD mice. (**F**) Quantification of m6A levels within microglia. N=3 or 4 biological replicates for each group. (**G**) Quantification of relative expression level of m6A-related genes in WT and 5xFAD microglia. Two-tailed independent t test, $p<0.05$. (**H**) Immunofluorescence staining showed $IBA1^{+}ALKNH5^{+}$ cells around Aβ region and non-Aβ region. (**I**) Statistics of the number of $IBA1^{+}ALKBH5^{+}$cells around Aβ region and non-Aβ region. Scale bar is 50 μm.

Supplementary Files

This is a list of supplementary files associated with this preprint. Click to download.

- sf1.tif
- sf2.tif
- sf3.tif
- sf4.tif
- sf5.tif
- sf6.tif
- sf7.tif
- supplementarytable1qPCRrawdata.xlsx
- supplementarytable25FADvsCtrldiffPeakexpression.xlsx
- supplementarytable3diffpeakKEGGandGOBPresults.xlsx
- supplementarytable4m6Adownupandgenedownuplists.xlsx
- supplementarytable54quartantKEGGandGOBPresults.xlsx
- supplementarytable6primerantibodyusedinthisstudy.xlsx